© 2024 Journal of Pharmacy & Pharmacognosy Research, 12 (1), 73-90, 2024
ISSN 0719-4250
https://jppres.com

DOI: https://doi.org/10.56499/jppres23.1735_12.1.73

Original Article

Structure elucidation of active compounds from *Coffea canephora* Pierre ex A.Froehner cascara and their potential as anticancer against breast cancer cells

[Elucidación estructural de compuestos activos de la cáscara de *Coffea canephora* Pierre ex A.Froehner y su potencial como anticancerígeno contra células de cáncer de mama]

Novi Fajar Utami[1,2], Berna Elya[1*], Hayun[1], Kusmardi Kusmardi[3,4,5]

[1]Department of Phytochemistry and Pharmacognosy, Faculty of Pharmacy, Universitas Indonesia, Depok 16424 West Java, Indonesia.
[2]Faculty of Math and Science, Universitas Pakuan, Jl. Raya Pakuan 1 Bogor, Indonesia.
[3]Department of Anatomic Pathology, Faculty of Medicine, Universitas Indonesia, Jl. Salemba Raya No.6, Jakarta, 10430, Jakarta, Indonesia, 10430 Indonesia.
[4]Drug Development Research Cluster, Indonesia Medical Educational and Research Institute, Jl. Salemba Raya No.6, Jakarta 10340, Indonesia.
[5]Human Cancer Research Cluster, Indonesia Medical Educational and Research Institute, Jl. Salemba Raya No.6, Jakarta 10340, Indonesia.
*E-mail: berna.elya@famasi.ui.ac.id

Abstract

Context: One approach to cancer therapy medication is exploring medicinal plants that contain one or more compounds specifically targeting cancer cells with fewer side effects. Cascara from coffee fruit (*Coffea canephora* Pierre ex A.Froehner) is a waste rarely processed but has various chemical contents that can be used in medicine.

Aims: To evaluate the *in silico* and *in vitro* activity of compounds isolated from ethanolic extract of *C. canephora* cascara against HeLa and MCF-7 breast cancer cells.

Methods: Isolation of the compounds by radial chromatography and thin layer chromatography techniques, and the chemical structures were elucidated by infrared radiation, ultraviolet, nuclear magnetic resonance spectroscopy, and mass spectrometry. *In silico* study about the compounds binding with the receptor responsibility to cancer (caspases 3 and 9). *In vitro* study by examining the cytotoxicity of HeLa and MCF-7 cells of the isolated compounds from *C. canephora*.

Results: Four known bioactive compounds, lupeol (1), stigmasterol (2), ursolic acid (3), and caffeic acid (4), were isolated from the ethanol extract of *C. canephora* cascara. Based on the ESI-MS results, the m/z value for lupeol was 427.50 $[M+H]^+$, stigmasterol was 454.48 $[M+ACN+H]^+$, ursolic acid was 456.51 $[M+H]^+$, and caffeic acid was 179 [M-H]. *In silico* and *in vitro* data show that the ursolic acid compound has activity against HeLa and MCF-7 cancer cells with IC_{50} values of 25.98 ± 0.01 µg/mL and 12.70 ± 0.11 µg/mL, respectively.

Conclusions: All isolated compounds from *C. canephora* cascara have a promising ability to interact with caspases 3 and 9, particularly ursolic acid, which has the smallest IC_{50} value against HeLa and MCF-7 breast cancer cells.

Keywords: cancer; cascara; cytotoxicity; *in silico*; *in vitro*; peel.

Resumen

Contexto: Uno de los enfoques de la medicación para el tratamiento del cáncer es la exploración de plantas medicinales que contengan uno o más compuestos dirigidos específicamente contra las células cancerosas con menos efectos secundarios. La cáscara del fruto del café (*Coffea canephora* Pierre ex A.Froehner) es un residuo raramente procesado pero tiene diversos contenidos químicos que pueden utilizarse en medicina.

Objetivos: Evaluar la actividad *in silico* e *in vitro* de los compuestos aislados del extracto etanólico de la cáscara de *C. canephora* frente a células de cáncer de mama HeLa y MCF-7.

Métodos: Aislamiento de los compuestos mediante técnicas de cromatografía radial y cromatografía en capa fina, y las estructuras químicas se dilucidaron mediante radiación infrarroja, ultravioleta, espectroscopia de resonancia magnética nuclear y espectrometría de masas. Estudio *in silico* sobre la unión de los compuestos con el receptor responsable del cáncer (caspasas 3 y 9). Estudio *in vitro* examinando la citotoxicidad de las células HeLa y MCF-7 de los compuestos aislados de *C. canephora*.

Resultados: Se aislaron cuatro compuestos bioactivos conocidos, lupeol (1), estigmasterol (2), ácido ursólico (3) y ácido cafeico (4), a partir del extracto etanólico de la cáscara de *C. canephora*. Según los resultados de la ESI-MS, el valor m/z del lupeol fue de 427,50 [M+H]+, el del estigmasterol fue de 454,48 [M+ACN+H]+, el del ácido ursólico fue de 456,51 [M+H]+, y el del ácido cafeico fue de 179 [M-H]. Los datos *in silico* e *in vitro* muestran que el compuesto de ácido ursólico tiene actividad contra las células cancerosas HeLa y MCF-7 con valores de IC_{50} de 25,98 ± 0,01 µg/mL y 12,70 ± 0,11 µg/mL, respectivamente.

Conclusiones: Todos los compuestos aislados de la cáscara de *C. canephora* tienen una prometedora capacidad para interaccionar con las caspasas 3 y 9, en particular el ácido ursólico, que presenta el menor valor de IC_{50} frente a las células de cáncer de mama HeLa y MCF-7.

Palabras Clave: cáncer; cáscara; citotoxicidad; *in silico*; *in vitro*.

ARTICLE INFO
Received: July 5 3, 2023.
Accepted: October 8, 2023.
Available Online: November 13, 2023.

AUTHOR INFO
ORCID:
0009-0005-4564-4584 (NFU)
0000-0002-1495-6228 (H)
0000-0003-2904-6515 (BE)
0000-0003-4380-723X (KK)

INTRODUCTION

Cancer is one of the diseases caused by perpetual genetic mutations until the alteration of cell function due to the abnormality of some genes (Schegoleva et al., 2022). Mutation of cancer cells is caused by some factors, for instance, radiation of X-rays, UV rays, high exposure to radioactive substances, carcinogenic substances, and viruses (Melosky et al., 2022). Based on WHO data in 2020, cancer is one of the biggest mortality rates caused by many factors (Giaquinto et al., 2022).

There are some medications related to the manifestation of cancer therapy: surgical therapy, radiation, chemotherapy, immunotherapy, and targeted medicines. Recently, chemotherapy and radiation have been generally applied, yet there were some side effects and resistance to these therapies (Li et al., 2022; Love et al., 1989). As time goes by, researchers develop other approaches to cancer therapy medication. One is by exploring medicinal plants that contain one or more compounds specifically targeting cancer cells with fewer side effects (Li et al., 2022). Therefore, the challenge of continually searching for new cancer drugs with diverse chemical structures that can effectively combat cancer cells and have low side effects remains essential, including through the exploration of natural substances, primarily from plants (botanical raw materials) (Li et al., 2022). Botanical raw materials that have been proven to have anticancer properties include species of coffee plants (*Coffea* sp) (Gallardo-Ignacio et al., 2022).

Coffea canephora Pierre ex A.Froehner (family *Rubiaceae*) has anticancer properties (Gallardo-Ignacio et al., 2022). In coffee cultivation, around 50-60% of cascara waste is generated (Rios et al., 2020). Recently, processed cascara has been produced as food and supplement products because it contains proteins, polysaccharides, and active compounds (Klingel et al., 2020). This will be a promising approach to developing cancer therapy that can be targeted specifically to cancer cells without affecting the normal cells in the body. According to Yashin et al. (2017), some compound contents found in coffee beans are also present in the coffee cascara, making it an opportunity for initial testing and development of the potential anticancer properties of coffee cascara, particularly from *Robusta* coffee varieties (Duangjai et al., 2016; Durán-Aranguren et al., 2021).

The process of designing, discovering, and optimizing bioactive compounds in the development of a new drug can be facilitated through *in silico* methods. *In silico* represents a fast and cost-effective way to identify new drugs. *In silico* is an effective method to identify the activity of many compounds isolated from plants to the targeted receptor using software (Hardjono et al., 2016; Nur et al., 2023). This method is useful for screening secondary metabolites isolated from coffee as a preliminary approach for further experiments. This study aimed to evaluate the *in silico* and *in vitro* activity of compounds isolated from ethanolic extract of *C. canephora* cascara against HeLa and MCF-7 breast cancer cells.

MATERIAL AND METHODS

Plant material

The plant material fruit cascara of *Coffea canephora* Pierre ex A.Froehner was used as plant material. They were taken from Bogor regency, West Java, Indonesia (lat -6.74238°, long 107.006648°), and their identities were verified at Herbarium Bogoriensis, BRIN Cibinong, Indonesia (B-483/V/D1.05.07/10/2021).

Materials

ChemOffice v8.0, HyperChem Release v8.07, Discovery Studio Visualizer v4.5, and DOCK 6 software programs were purchased from UCSF (University of California, San Fransisco). FT-IR Spectrometer Nicolet iS50, Biosafety Cabinet (BSC) Class II 1300 series type A2, MicroCL17 microcentrifuge, CO_2 incubator 8000 DH series, and Microscope (EVOS XL Core) were purchased from Thermo Fisher Scientific (USA). The compounds' mass was recorded using TQD LCMS-Ultra Performance Liquid Chromatography (UPLC) (Waters, USA). 1-D and 2-D NMR 500 MHz CryoProbe from Bruker (USA). Radial chromatography for isolation was performed using round glass plates Kieselgel 60 PF254 (art. no. 7749) and TLC silica gel 60 F254 of 0.25 mm thickness (art. no. 5554) from Merck (USA). Cytotoxicity test was carried out using a 96-well plate (Nest Scientific, USA), micropipettes, and tips (Mettler Toledo, USA).

Chemical and reagents

Chemicals such as $CeSO_4$, ethanol, n-hexane, ethyl acetate, and EDTA were purchased from Merck, USA. DMEM media, FBS, antibiotic penicillin-streptomycin, trypsin, trypan blue from Gibco, USA. HeLa and MCF-7 cell lines from ATCC, PrestoBlue cell viability reagent from Invitrogen, USA, and cisplatin and DMSO were purchased from Sigma-Aldrich, USA.

Extraction and isolation of the active compounds from *C. canephora*

Preventive parading

C. canephora fruits were cleaned with water and cut into small pieces, then next were air-dried to give 5.0 kg of dry sample. The dried sample was ground and extracted with 70% ethanol (EtOH). After filtration, the extract was dried in a vacuum at 45°C to give a crude extract. Fractionation of the extract was carried out with vacuum liquid chromatography (VLC) using a column (80 mm id × 500 mm) of silica gel (7734). The mobile phase was n-hexane/ethyl acetate (EtOAc) with increased polarity. Radial chromatography (RC) was utilized for the purification process, using 95:5 n-hexane-EtOAc in 10% polarity increment to weight compounds **1** (25 mg), **2** (14 mg), **3** (18 mg) and **4** (32 mg) (Rosandy et al., 2018).

Active compounds analysis

(1) Lupeol

White amorphous; m.p 215-217° C; ESIMS [M+H]+ m/z 427; **^{1}H NMR (Chloroform-d, 500 MHz)** δH: 1.61 (2H, t, H-1), 1.63 (2H, m, H-2), 3.19 (1H, dd, 10.8, 5.4, H-3), 0.69 (1H, d, 9.0, H-5), 1.39 (2H, m, H-6), 1.39 (2H, t, 9.0, H-7), 1.27 (1H, t, 5.4, H-9), 1.39 (2H, m, H-11), 1.27 (2H, m, H-12), 1.69 (1H, t, 6.6, H-13) 1.69 (1H, t, 6.6, H-15), 1.52 (1H, m, H-16a), 1.47 (1H, m, H-16b), 1.39 (1H, t, 9.0, H-18), 2.38 (1H, m, H-19), 1.92 (1H, m, H-21a), 1.27 (1H, m, H-21b), 1.63 (2H, t, H-22), 0.97 (3H, s, H-23), 0.77 (3H, s, H-24), 0.84 (3H, s, H-25), 1.04 (3H, s, H-26), 0.95 (3H, s, H-27), 0.79 (3H, s, H-28), 4.70 (1H, s, H-29a), 4.57 (1H, s, H-29b), 1.69 (3H, s, H-30); **^{13}C NMR (Chloroform-d, 125 MHz) δH**: 38.7 (C-1), 27.5 (C-2), 78.9 (C-3), 38.9 (C-4), 55.3 (C-5), 18.3 (C-6), 34.3 (C-7), 40.8 (C-8), 50.4 (C-9), 37.1 (C-10), 20.9 (C-11), 25.2 (C-12), 38.1 (C-13), 42.9 (C-14), 27.4 (C-15), 35.6 (C-16), 48.2 (C-17), 48.3 (C-18), 47.9 (C-19), 150.9 (C-20), 29.9 (C-21), 40.0 (C-22), 28.0 (C-23), 15.4 (C-24), 16.1 (C-25), 16.0 (C-26), 14.6 (C-27), 18.0 (C-28), 109.4 (C-29), 19.3 (C-30). See Fig. S1.

(2) Stigmasterol

Colorless crystal; m.p 134-136°C; ESIMS [M+H]+ m/z 413; **^{1}H NMR (Chloroform-d, 500 MHz) δH**: 1.84 (2H, m, H-1), 1.51 (2H, m, H-2), 3.51 (1H, m, H-3), 2.24 (2H, dd, 10.5, 2.1, H-4), 5.34 (1H, d, 5.4, H-6), 1.84 (2H, m, H-7), 1.93 (1H, m, H-8), 1.44 (1H, m, H-9), 1.47 (2H, m, H-11), 2.00 (2H, dd, 9.3, 3.0, H-12) 1.10 (1H, m, H-14), 1.55 (2H, m, H-15), 1.25 (2H, m, H-16), 1.07 (1H, m, H-17), 0.68 (3H, s, H-18), 0.99 (3H, s, H-19), 1.99 (1H, m, H-20), 0.91 (3H, d, 6.3, H-21), 4.99 (1H, dd, 15.2, 8.7, H-22), 5.14 (1H, dd, 15.2, 8.7, H-23), 1.93 (1H, m, H-24), 1.65 (1H, m, H-25), 0.81 (3H, d, 6.5, H-26), 0.79 (3H, d, 6.5, H-27), 1.25 (2H, m, H-28) , 0.84 (3H, t, 3.3, H-29); **^{13}C NMR (Chloroform-d, 125 MHz) δH**: 37.0 (C-1), 31.7 (C-2), 71.5 (C-3), 42.0 (C-4), 140.5 (C-5), 121.5 (C-6), 31.4 (C-7), 31.6 (C-8), 49.9 (C-9), 36.3 (C-10), 20.9 (C-11), 39.5 (C-12), 42.1 (C-13), 56.5 (C-14), 24.1 (C-15), 28.0 (C-16), 55.8 (C-17), 11.6 (C-18), 18.8 (C-19), 40.3 (C-20), 18.6 (C-21), 138 (C-22), 129.0 (C-23), 51.0 (C-24), 28.9 (C-25), 19.6 (C-26), 19.2 (C-27), 22.8 (C-28), 11.7 (C-29). See Fig. S2.

(3) Ursolic acid

White amorphous; m.p 215-217°C; ESIMS [M+H]+ m/z 457; **^{1}H NMR (DMSO, 500 MHz) δH**: 1.0 (1H, 13.15, H-1a), 1.52 (1H, m, H-1b), 1.45 (2H, q, H-2), 3.00 (1H, m, H-3), 4.29 (1H, d, OH-3), 0.66 (1H, br-s, H-5), 1.45 (1H, m, H-6a), 1.29 (1H, m, H-6b), 1.42 (1H, m, H-7a), 1.26 (1H, m, H-7b), 1.44 (1H, t, 6.8, H-9), 1.85 (2H, t, 3.0, H-11), 5.13 (1H, t, 3.25, H-12), 1.80 (2H, m, H-15) 1.91 (1H, m, H-16a), 1.52 (1H, m, H-16b), 2.10 (1H, d, 11.25, H-18), 1.52 (1H, m, H-19), 1.28 (1H, m, H-20), 1.42 (2H, m, H-21), 1.54 (2H, m, H-22), 0.89 (3H, s, H-23), 0.68 (3H, s, H-24), 0.87 (3H, s, H-25), 0.75 (3H, s, H-26), 1.04 (3H, s, H-27), 11.93 (1H, s, OH-28), 0.80 (3H, d, 6.45 H-29), 0.89 (3H, d, H-30); **^{13}C NMR (DMSO, 125 MHz) δH**: 39.2 (C-1), 28.2 (C-2), 78.2 (C-3), 39.6 (C-4), 55.9 (C-5), 18.8 (C-6), 33.7 (C-7), 40.1 (C-8), 48.1 (C-9), 37.5 (C-10), 23.7 (C-11), 125.7 (C-12), 139.3 (C-13), 42.6 (C-14), 28.8 (C-15), 25.0 (C-16), 48.1 (C-17), 53.6 (C-18), 39.5 (C-19), 39.4 (C-20), 31.1 (C-21), 37.4 (C-22), 28.8 (C-23), 16.5 (C-24), 15.7 (C-25), 17.5 (C-26), 24.0 (C-27), 179.7 (C-28), 17.5 (C-29), 21.4 (C-30). See Fig. S3.

(4) Caffeic acid

White amorphous; m.p 235-236°C; ESIMS [M+H]+ m/z 181; UV λmax (MeOH) nm (log ε): 203.53 and 340.51 nm; **^{1}H NMR (DMSO, 500 MHz) δH**: 6.98 (1H, d, 2.0 Hz, H-2), 6.71 (1H, d, 8.16 Hz, H-5), 6.92 (1H, dd, 8.16, 2.12 Hz, H-6), 7.37 (1H, d, 15.88 Hz, H-7), 6.12 (1H, d, 15.92 Hz, H-8), 12.06 (1H, s, 9-OH), 9.47 (1H, s, 3-OH), 9.07 (1H s, 4-OH); **^{13}C NMR (DMSO, 125 MHz) δH**: 126.22 (C-1), 115.16 (C-2), 146.08 (C-3), 148.66 (C-4), 116.26 (C-5), 121.67 (C-6), 145.12 (C-7), 115.63 (C-8), 168.42 (C-9). See Fig. S4.

Culture cell conditions and cytotoxic assay

The cytotoxicity of compounds **1–4** was determined with a cell viability test using PrestoBlue® assay. The cells were maintained in a Roswell Park Memorial Institute (RPMI) medium with 10% (v/v) Fetal Bovine Serum (FBS) and 1 µL/1 mL antibiotics (1% penicillin–streptomycin). Cultures were incubated at 37°C in a humidified atmosphere of 5% CO_2 (Aisyah et al., 2022; Nur et al., 2021). MCF-7 cells were plated in 96 multiwell culture plates at a density of 1.7

× 10^4 cells/well. After twenty-four hours, the medium was discarded, and fresh medium containing samples (*C. canephora* extracts, fractions, and isolates) with different concentrations of 7.81, 15.63, 31.25, 62.50, 125.00, 250.00, 500.00, 1000.00 µg/mL and with the positive control cisplatin. After incubation with the sample for 24 h, PrestoBlue® reagent (resazurin dye) was added. The PrestoBlue® assay results were read using a multimode reader at 570 nm (Tecan Infinite M200 PRO, Switzerland). The IC_{50} value was determined by linear regression using Microsoft Excel software. Then, the IC_{50} value was calculated as the extract concentration that inhibited cell viability by 50% after the exposure time. The selectivity index (SI) was defined as the ratio of the IC_{50} value observed against cancer cell lines to the IC_{50} value observed in non-malignant cells (Céspedes et al., 2023).

In silico screening of bioactive compounds

Preparation of ligand structure

To create ligand structures, including lupeol, stigmasterol, ursolic acid, caffeic acid, and cisplatin as reference compounds, began with designing the 2D form by using the ChemDraw Ultra 8.0 program inside the package ChemOffice v8.0 program. Then, to 3D form by using Chem3D v8.0 on the same package. The file was saved in *mol format. The 3D structure was optimized geometrically by using the HyperChem Release v8.07 program. The optimization of the tested compounds was carried out by the software Chimera for the addition of hydrogen and charges, and then the file was saved as *. mol2 format for further docking process by using the DOCK 6 program (Nursamsiar et al., 2022).

Preparation of molecules

The 3D structures of caspases 3 and 9 target proteins were displayed in the package Discovery Studio Visualizer v4.5 program. Chain B (caspase 3) and chain A (caspase 9), as the receptor, were separated from water molecules and other of their native ligands and then saved as *.pdb format. By operating the Chimera program, hydrogen, and charges were added to the protein structure, then the file was saved as *. mol2 format for further docking process by using the DOCK 6 program (Nur et al., 2023; Nursamsiar et al., 2020).

Validation of docking method

Validation was conducted by re-docking its native ligands into the active side of the receptors/proteins. The Relative Mean Standard Deviation (RMSD) determined the method's validity. If the score is less than 2, the docking method is valid and ready to be attached to the tested compounds (Nur et al., 2023).

Docking simulation

The docking simulation of tested compounds was performed using the DOCK 6 program and visualized by Chimera (UCSF, 2023). Both caspase 3 and 9 were prepared without hydrogen atoms to determine the spheres around the protein surface. The identification of spheres is based on the location of the natural ligands by the RMSD, about 8 Å each atom. After sphere identification, the grid box area and the size of the natural ligand binding site were determined in the margin of 5 Å. Energy minimization was applied to the optimized ligand compounds from *C. canephora* and cisplatin as reference compounds before the docking process, while the docking process was next performed by the rigid-docking method. The *in silico* evaluation parameters regarding the ligand structure's orientation to the protein target, hydrophobic interaction, the formation of hydrogen bonds, and the grid score of docking processes from each ligand were evaluated.

Statistical analysis

Data were expressed as the mean ± standard deviation of at least two experiments and analyzed using the GraphPad Prism 5 (2007) program (GraphPad Software, Inc.). Normality was tested using the Kolmo Gorov-Smirnov test, followed by the Bartlett or maximum F test to assess homogeneity. Duncan's multiple-range assay was used to analyze the kinetic characterization data of the culture medium. When significant differences were found, comparisons of means between treatments were performed using simple categorical analysis of variance (ANOVA) plus Dunnett's parametric post hoc test. $P<0.05$ was indicated as statistically significant.

RESULTS AND DISCUSSION

NMR data of isolated compounds

Compound **1** was isolated as a white amorphous solid. The molecular formula is $C_{30}H_{51}O$, and it was generated using ESI-MS [M+H]+ at m/z 427.50. The UV spectrum showed only one absorbance peak at 203.53 nm, indicating the absence of a conjugated system of double bonds. The FTIR spectrum showed a broad absorbance peak at $\bar{\upsilon}$ of 3367 cm^{-1}, indicating the stretching vibration of the O-H bond, and the vibration band of C-O bending was observed at 1040 cm^{-1}. The absorbance peak at 761 cm^{-1} indicated the out-of-plane bending vibration of O-H. The Csp3-H stretching bands appeared at 2943 and 2870 cm^{-1}.

Bending vibrations of Csp3-H of the methyl groups gave absorbance at 1457 (asymmetrical) and 1382 cm^{-1} (symmetrical), while the methylene rocking bending vibration band appeared at 720 cm^{-1}. The olefinic group was detected in this compound, shown by an absorbance peak of symmetrical C=C stretching at 1641 cm^{-1}. The absorption band at 3072 cm^{-1} indicated the vibration of the C sp2- H stretch, and the peak at 882 cm^{-1} explained that this compound contains vinyl-type double bond 1 and exhibited 30 carbons, which were identified using ^{13}C NMR. It was revealed that the compound was formed by seven methyls, 11 methylenes, six methines, and six quarternary carbons. The Double Bond Equivalent (DBE) value of six indicated that this compound was a pentacyclic triterpene with only one double bond. A carbon at δC 78.9 (C-3) showed the presence of an oxygen-attaching carbon, while the sole double bond in the molecule was shown by a pair of carbons at δC 150.9 (C-20) and 109.4 (C-29). Seven singlet methyls were detected in this compound, suggesting that all the methyl groups were attached to quarternary carbons. From the ^{1}H NMR, it was observed that there was a proton at δH 3.19 (dd, J = 10.8 and 5.4, H-3) integrating for one proton, indicating a proton attached to an oxygen-attaching carbon, which in this case was C-3. In addition, there were no carbon and proton signals with chemical shifts indicating a methoxy group. Thus, it can be concluded that C-3 attached a hydroxyl (-OH) instead of a methoxy group. Two highly deshielded protons at δH 4.70 and 4.57 (H-29) were attached to the same carbon (C-29). This explains that the highly deshielded carbon was a methylene group forming a double bond with a quarternary carbon (C-20). When a double bond in a triterpene molecule is formed by methylene and a quarternary carbon, it is confirmed outside the ring system. This skeletal characteristic belongs to the lupane-type triterpene lupeol (Rosandy et al., 2021). See Fig. S1.

Compound **2** was obtained as a colorless needle crystal. Only one absorbance peak was observed in the UV spectrum at 204.03 nm. This indicated the absence of a conjugated double bond in the molecule. The FTIR spectral data showed the stretching vibration band of O-H at 3431 cm^{-1}, C-O bends at 1052 cm^{-1}, and the out-of-plane bending vibration of O-H at 803 cm^{-1}. The peaks of stretching Csp3-H appeared at 2958, 2937, and 2869 cm^{-1}, while the bending vibrations of Csp3-H of the methyl groups gave absorption at 1464 (asymmetrical) and 1380 cm^{-1} (symmetrical). An absorbance peak of symmetrical stretching C=C at 1645 cm^{-1} indicated the existence of the olefinic group in this compound. The structure of **2** was further determined using ^{13}C and ^{1}H NMR spectral data. The carbon experiment showed that this compound contained 29 carbons of six methyls, nine methylenes, 11 methines, and three quarternary carbons. A methine carbon at δC 71.5 (C-3) indicated a carbon attached to an oxygen atom (oxymethine), revealing a hydroxyl group's existence. The presence of two pairs of highly deshielded carbons at δC 140.5 (C-5), 121.5 (C-6), 138.1 (C-22), and 129.0 (C-23) suggested that there were two double bonds in the molecule. The DBE value of six suggests that this compound was a tetracyclic compound containing two double bonds. The ^{1}H NMR experiment of **2** (Fig. 1) displayed information on the presence of two singlet methyl signals at δH 0.68 (H-18) and 0.99 (H-19), indicating that they were bound directly to the ring system. Three doublet methyls at δH 0.91 (H-21), 0.81 (H-26), and 0.79 (H-27), and one triplet methyl at δH 0.84 (H-29) were located at the side chain outside the rings of the main skeleton. A proton at δH 3.51 (H-3) was attached to the oxygen-binding carbon (C-3). The occurrence of three highly deshielded protons at δH 5.34 (H-6), 4.99 (H-22), and 5.14 (H-23) indicated the presence of two pairs of double bonds. The typical signal for the olefinic H-6 of the steroidal skeleton was evident from a proton at δH 5.34 integrating for one proton. The similar coupling constants (J = 15.2 Hz) of the other olefinic protons, H-22 and H-23, revealed that they were neighbors and were in transposition. Based on the discussion above and data comparison with the literature, compound **2** was identified as stigmasterol (Astuti et al., 2022). See Fig. S2.

Compound **3** was obtained as a colorless needle crystal. Only one absorbance peak was observed in the UV spectrum at 204.03 nm. This indicated the absence of a conjugated double bond in the molecule. The FTIR spectral data showed the stretching vibration band of O-H at 3431 cm^{-1}, C-O bends at 1052 cm^{-1}, and the out-of-plane bending vibration of O-H at 803 cm^{-1}. The peaks of stretching Csp3-H appeared at 2958, 2937, and 2869 cm^{-1}, while the bending vibrations of Csp3-H of the methyl groups gave absorption at 1464 (asymmetrical) and 1380 cm^{-1} (symmetrical). An absorbance peak of symmetrical stretching C=C at 1645 cm^{-1} indicated the existence of the olefinic group in this compound. The structure of compound **3** was further determined using ^{13}C and ^{1}H NMR spectral data. The carbon experiment showed that this compound contained 29 carbons of six methyls, nine methylenes, 11 methines, and three quarternary carbons. A methine carbon at δC 71.5 (C-3) indicated a carbon attached to an oxygen atom (oxymethine), revealing a hydroxyl group's existence. The presence of two pairs of highly deshielded carbons at δC 140.5 (C-5), 121.5 (C-6), 138.1 (C-22), and 129.0 (C-23) suggested that there were two double bonds in the molecule. The DBE value of six suggested that this compound was a tetracyclic compound containing two double bonds. The ^{1}H NMR experiment of **3** (Fig. 1)

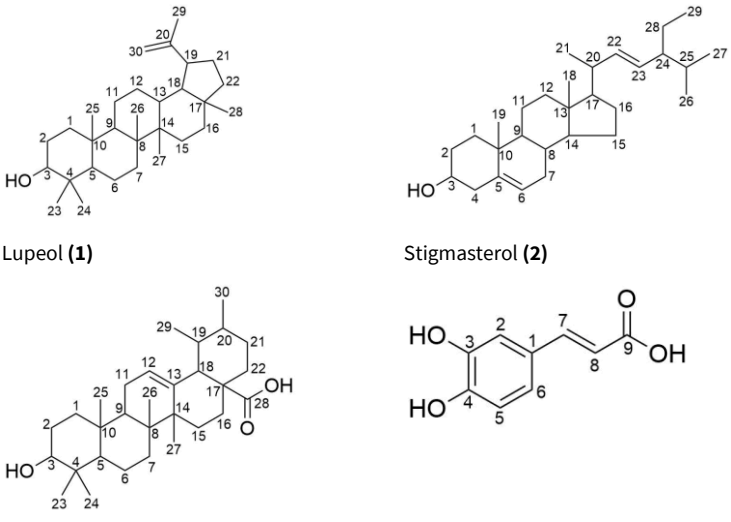

Lupeol **(1)**

Stigmasterol **(2)**

Ursolic acid **(3)**

Caffeic acid **(4)**

Figure 1. Chemical structure of isolated compounds from *C. canephora* cascara.

displayed information on the presence of two singlet methyl signals at δH 0.68 (H-18) and 0.99 (H-19), indicating that they were bound directly to the ring system. Three doublet methyls at δH 0.91 (H-21), 0.81 (H-26), and 0.79 (H-27), and one triplet methyl at δH 0.84 (H-29) were located at the side chain outside the rings of the main skeleton. A proton at δH 3.51 (H-3) was attached to the oxygen-binding carbon (C-3).The occurrence of three highly deshielded protons at δH 5.34 (H-6), 4.99 (H-22), and 5.14 (H-23) indicated the presence of two pairs of double bonds. The typical signal for the olefinic H-6 of the steroidal skeleton was evident from a proton at δH 5.34 integrating for one proton. The similar coupling constants (J = 15.2 Hz) of the other olefinic protons, H-22 and H-23, revealed that they were neighbors and were in transposition. Based on the discussion above and data comparison with the literature, compound **3** was identified as ursolic acid (Tan et al., 2019). See Fig. S3.

Compound **4** was isolated as a white amorphous solid. Its molecular formula was determined as $C_9H_7O_4$, obtained by ESI–MS [M - H]- m/z 179. The IR spectrum showed the presence of carbonyl groups (1735 cm^{-1}), -OH (3441 cm^{-1}), and -C=C- (1600-1450 cm^{-1}). The ^{13}C NMR spectrum showed the location of nine signals representing five methines and four quaternary carbons. The DBE value of six indicated that this compound contained five double bonds and one ring. The carbonyl group was indicated as the most deshielded carbon at δC 168.42 (C-9) ppm. Two non-equivalent olefinic methine signals at δC 145.12 (C-7) and 115.63 (C-8) ppm were attributed to the outside ring. Another six olefinic carbon signals at δC 126.22 (C-1), 115.16 (C-2), 146.08 (C-3), 148.66 (C-4), 116.26 (C-5), 121.67 (C-6) ppm to form an aromatic ring in this molecule. Meanwhile, eight proton signals representing eight protons appeared in the ^1H-NMR spectrum. Five signals came from the five non-equivalent olefinic protons at H-2, 3-OH, 4-OH, H-5, and H-6, forming 3,4-dihydroxy benzene. Two methine protons at δH 7.37 (^1H, d, 15.88 Hz, H-7) and 6.12 (^1H, d, 15.92 Hz, H-8), indicating that both protons were adjacent to forming trans-olefinic methine. The last signal was hydroxy at δH 12.06 (^1H, s, 9-OH) attached to carbonyl C-9. A comparison of the compound's ^{13}C and ^1H NMR spectra suggested it was caffeic acid (Silva et al., 2021). See Fig. S4.

In silico test of active compounds

Redocking results over receptors of caspases 3 and 9 using DOCK showed RMSD scores of 0.87 Å and 0.64 Å, respectively. RMSD score is one validation reference to assess the accuracy of the docked geometric poses with their crystallographic conformations (Adianingsih et al., 2022; Nur et al., 2023). The result showed valid by RMSD <2 Å (Ramírez and Caballero, 2018). The redocking result of natural ligands caspases 3 and 9 is shown in Fig. 2. It showed that the natural ligand poses due to redocking coincide (shown in gray color) with their crystallographic poses (red). The function score used in the DOCK 6 program is the grid score, and the attachment score is shown in Table 1. The figure of redocking of the natural ligands of caspases 3 and 9 are shown in Fig. 3.

Hydrogen bond spacing had a role to determine the inhibitory activity of a ligand. A strong hydrogen bond might be proportional to a very weak covalent bond. The hydrogen bond with the gap of donor-acceptor 1.2 – 1.5 Å was categorized as a strong bond, whereas the gap of 1.5 – 2.2 Å was categorized as a

moderate bond, and 2.2 - 3.2 Å was categorized as a weak bond (Adianingsih et al., 2022; Riwu et al., 2022). The interaction and bond distance of each compound with its receptor are shown in Tables 2 and 3. Visualization of molecular attachment to caspases 3 and 9 receptors is shown in Figs. 3 and 4.

A prediction study of compound interaction with caspase-3 (PDB ID: 1PAU) and 9 (PDB ID: 1JXQ) was conducted by molecular attachment study by running the protocol DOCK 6 with the method of flexible ligand docking. The ligand is freely moved in this method, yet the receptor remains rigid. This method is widely used due to its accuracy, which is more than the rigid docking method, where the flexible ligand docking method gives more ligand confirmation of interaction. DOCK molecular attachment was validated based on root mean square deviation (RMSD) from the redocking result of the natural ligand of caspases 3 and 9.

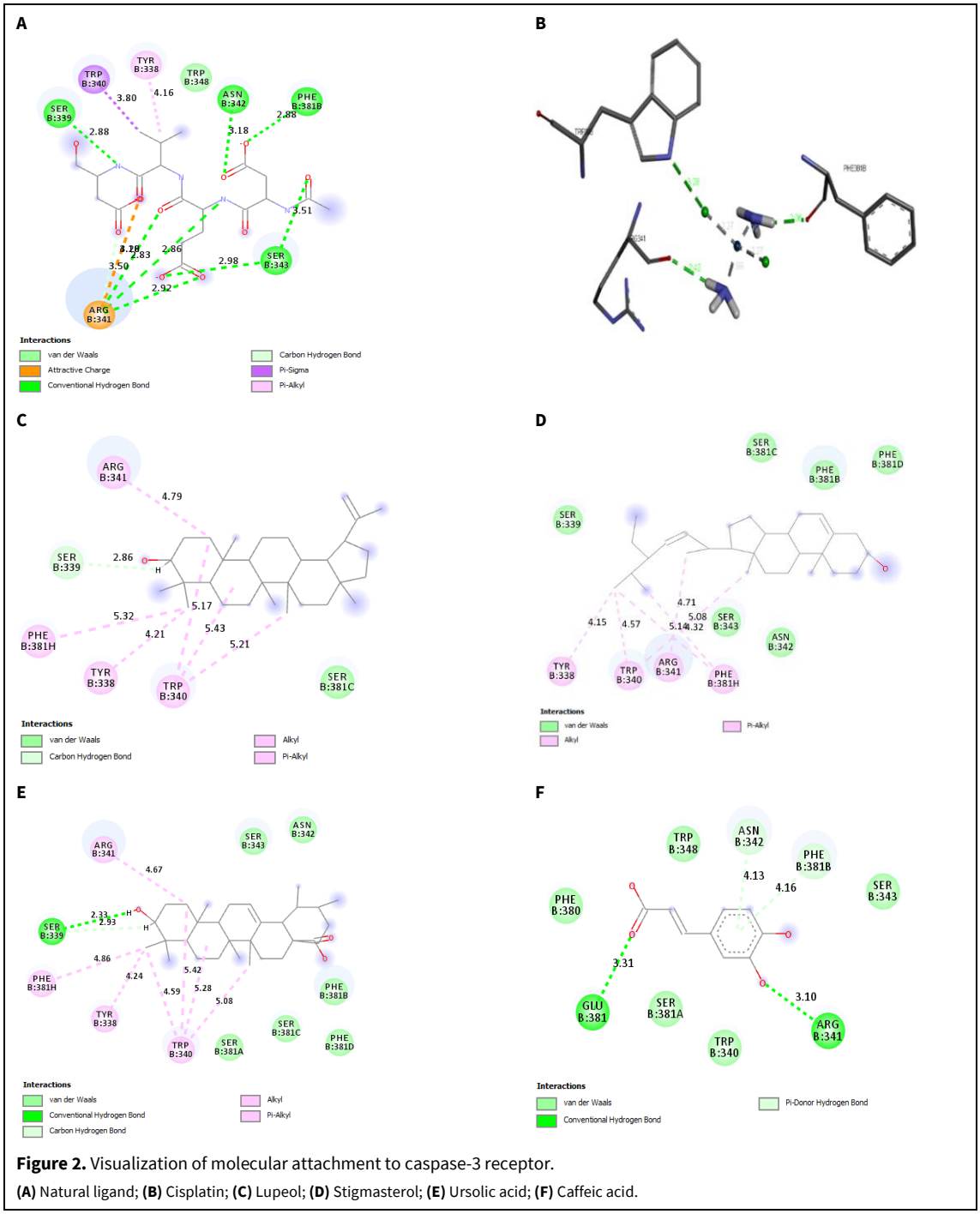

Figure 2. Visualization of molecular attachment to caspase-3 receptor.
(A) Natural ligand; **(B)** Cisplatin; **(C)** Lupeol; **(D)** Stigmasterol; **(E)** Ursolic acid; **(F)** Caffeic acid.

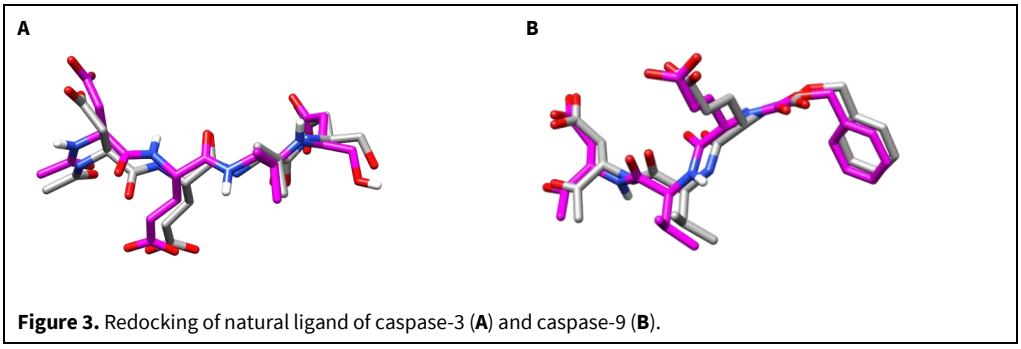

Figure 3. Redocking of natural ligand of caspase-3 (**A**) and caspase-9 (**B**).

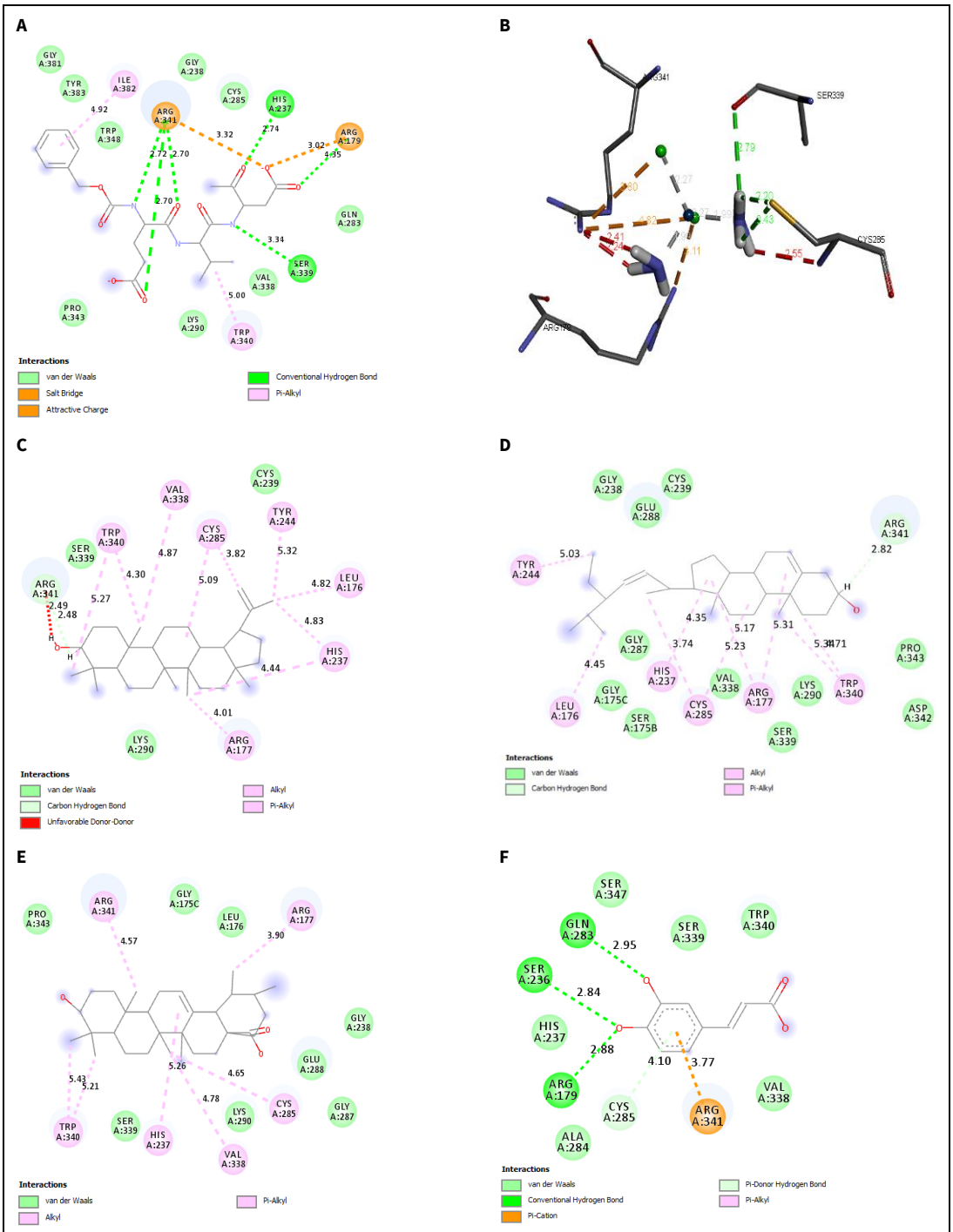

Figure 4. Visualization of molecular attachment to caspase-9 receptor.

(A) Natural ligand; **(B)** Cisplatin; **(C)** Lupeol; **(D)** Stigmasterol; **(E)** Ursolic acid; **(F)** Caffeic acid.

Table 1. Attachment score of all compounds to caspases 3 and 9.

Receptors	Compound	Attachment score (kcal/mol)
Caspase 3 (PDB ID: 1PAU)	Natural ligand	-76.36
	Cisplatin	-13.88
	Lupeol (**1**)	-41.36
	Stigmasterol (**2**)	-39.14
	Ursolic acid (**3**)	-43,67
	Caffeic acid (**4**)	-21,57
Caspase 9 (PDB ID: 1JXQ)	Natural ligand	-86,05
	Cisplatin	-16,24
	Lupeol (**1**)	-43.47
	Stigmasterol (**2**)	-43,22
	Ursolic acid (**3**)	-45,10
	Caffeic acid (**4**)	-29,02

Table 2. Compound interaction with caspase 3 receptor (PDB ID: 1PAU).

Ligands	Amino acid residue and its bond distance (Å)		
	Hydrogen bond	**Hydrophobic interaction**	**Electrostatic interaction**
Natural ligand	Arg341 (2,83; 2,86; 2,92; 3,14; 3,50) Ser343 (2,98; 3,51) Phe381 (2,88) Asn342 (3,18) Ser339 (2,88)	Trp340 (3,80) Tyr338 (4,16)	Arg341 (4,20)
Cisplatin	Arg341 (2,42) Trp348 (3,28) Phe381 (2,06)		
Lupeol **(1)**	Ser339 (2,86)	Phe381 (5,32) Tyr338 (4,21) Trp340 (5,17; 5,21; 5,43) Arg341 (4,79)	
Stigmasterol **(2)**		Tyr338 (4,15) Trp340 (4,57; 5,08) Arg341 (4,71) Phe381 (4,32; 5,14)	
Ursolic acid **(3)**	Ser339 (2,33; 2,93)	Arg341 (4,67) Phe381 (4,86) Tyr338 (4,24) Trp340 (4,59; 5,08; 5,28; 5,42)	
Caffeic acid **(4)**	Arg341 (3,10) Glu381 (3,31) Asn342 (4,13) Phe381 (4,16)		

Table 3. Compound interaction with caspase 9 receptor (PDB ID: 1JXQ).

Ligands	Amino acid residues and its bond distance (Å)		
	Hydrogen bond	**Hydrophobic interaction**	**Electrostatic interaction**
Natural ligand	His237 (2,74) Arg341 (2,72; 2,70) Ser339 (3,34) Arg179 (4,35)	Ile382 (4,92) Trp340 (5,00)	Arg341 (3,32) Arg179 (3,02)
Cisplatin	Ser339 (2,79) Cys285 (2,20; 2,43)		Arg341 (3,80; 4,82) Arg179 (3,11)
Lupeol **(1)**	Arg341 (2,48)	Trp340 (4,30; 5,27) Val338 (4,87) Cys285 (3,82; 5,09) Tyr244 (5,32) Leu176 (4,82) His237 (4,44; 4,83) Arg177 (4,01)	
Stigmasterol **(2)**	Arg341 (2,82)	Tyr244 (5,03) Leu176 (4,45) His237 (4,35) Cys285 (3,74; 5,23) Arg177 (5,17; 5,31) Trp340 (5,34; 4,71)	
Ursolic acid **(3)**		Arg341 (4,57) Arg177 (3,90) Cys285 (4,65) Val338 (4,78) His237 (5,26) Trp340 (5,21; 5,43)	
Caffeic acid **(4)**	Ser236 (2,84) Arg179 (2,88) Gln283 (2,95) Cys285 (4,10)	Arg341 (4,94)	Arg341 (3,77)

Cytotoxic activities

By the cytotoxicity results of the compounds isolated from *C. canephora* cascara ethanolic extract, ursolic acid showed the smallest value of IC_{50} among the other compounds, even smaller than the positive control (cisplatin) on MCF-7 cells (Table 4). *In vitro* studies of ursolic acid have also been reported to inhibit the progression of breast cancer cells targeting the NF-κB pathway (Fitriana et al., 2022; Liu et al., 2015). Non-malignant cells were extracted to calculate the selectivity index (SI) with the IC_{50} value until a concentration of 1000 µg/mL, which was the maximum concentration evaluated. Based on the results, ursolic acid showed the highest selectivity against Hela cells and MCF-7 cells. Table 4 shows the IC_{50} level of some compounds derived from *C. canephora* cascara to HeLa and MCF-7 breast cancer cells.

According to an *in vitro* cytotoxicity assay of the four compounds isolated from *C. canephora* cascara, ursolic acid exhibited the smallest IC_{50} in both HeLa and MCF-7 cells. Ursolic acid is widely known to have activities against diseases, including anti-inflammatory, antimicrobial, antidiabetic, and anticancer. Some studies regarding its activity towards breast cancer have been reported, for example, by molecularly suppressing glycolytic metabolism via activation of Sp1/caveolin-1 signaling (Khochapong et al., 2021; Luzak et al., 2022). Since ursolic acid also interacts with caspases 3 and 9 in the present study. It could be understood that the small value of IC_{50} obtained from ursolic acid is based on its ability to perform cell apoptosis in cancer, particularly breast cancer.

Table 4. IC_{50} level of some compounds derived from cascara to HeLa and MCF-7 breast cancer cells.

Compound	IC_{50} (µg/mL) ± SD (SI)	
	Hela cells	**MCF-7 cells**
Extract	486.31 ± 0.17 (1.79)	412.57 ± 0.28 (2.04)
n-hexane fraction	121.59 ± 0.12 (2.5)	221.57 ± 0.12 (2.44)
Ethyl acetate fraction	99.36 ± 0.41 (2.22)	130.3 ± 0.23 (2.14)
Methanol fraction	323.07 ± 0.01 (1.75)	159.49 ± 0.16 (1.82)
Lupeol (**1**)	89.94 ± 0.46 (2.36)	96.53 ± 0.42 (1.96)
Stigmasterol (**2**)	94.94 ± 0.30 (2.33)	66.44 ± 0.29 (2.54)
Ursolic acid (**3**)	25.98 ± 0.01 (6.42)	12.70 ± 0.11 (7.63)
Caffeic acid (**4**)	102.98 ± 0.12 (3.81)	101.50 ± 0.23 (2.86)
Cisplatin (+ control)	9.05 ± 0.16 (8.28)	53.00 ± 0.11 (3.73)

The selectivity index (SI) was calculated by dividing the IC_{50} value of normal cells by the IC_{50} value of cancer cells. The SI value represents the sample selectivity of the cell lines tested.

CONCLUSION

The IC_{50} value of the compounds isolated from *C. canephora* cascara against HeLa and MCF-7 breast cancer and the correlation with *in silico* results towards interaction to caspases 3 and 9. It can be concluded that all of the compounds have potential for cancer therapy, particularly ursolic acid, which showed the smallest IC_{50} value against HeLa and MCF-7 breast cancer. More advanced approaches to getting a specific molecular target in cancer cells are needed.

CONFLICT OF INTEREST

The authors declare no conflicts of interest.

ACKNOWLEDGMENTS

This research did not receive any specific grant from funding agencies in the public, commercial, or not-for-profit sectors.

REFERENCES

Adianingsih OR, Khasanah U, Anandhy KD, Yurina V (2022) *In silico* ADME-T and molecular docking study of phytoconstituents from *Tithonia diversifolia* (Hemsl.) A. Gray on various targets of diabetic nephropathy. J Pharm Pharmacogn Res 10: 571–594. https://doi.org/10.56499/jppres22.1345.10.4.571

Aisyah A, Lukitaningsih E, Rumiyati R, Marwati M, Sapra A, Khairi N, Fadri A, Nur S (2022) *In vitro* antioxidant and cytotoxic evaluation of ethyl acetate fraction of *Angiopteris ferox* Copel tuber against HTB lung cancer cell. Egypt J Chem 65(11): 41–48. https://doi.org/10.21608/ejchem.2022.91843.4364

Astuti A, Yasir B, Rahim A, Natzir R, Subehan S, Goto K, Alam G (2022) Isolation and characterization of stigmasterol and β-sitosterol from *Plectranthus scutellarioides* var. color blaze dark star and cytotoxicity of its fraction. Egypt J Chem 65(3): 255–260. https://doi.org/10.21608/ejchem.2021.80171.3972

Céspedes I, Fuentes-León F, Rodeiro I, Laurencio-Lorca Y, Iglesias MV, Herrera JA, Cuellar C, Caballero V, Pereira L, Cuétara E, Sánchez A, Fernández MD, Núñez RR, Hernández-Balmaseda I, Ortiz E (2023) Kinetic characterization, antioxidant and *in vitro* toxicity potential evaluation of the extract M116 from *Bacillus amyloliquefaciens*, a Cuban southern coast marine microorganism. J Pharm Pharmacogn Res 11(4): 547–556. https://doi.org/10.56499/jppres23.1574_11.4.547

Duangjai A, Suphrom N, Wungrath J, Ontawong A, Nuengchamnong N, Yosboonruang A (2016) Comparison of antioxidant, antimicrobial activities and chemical profiles of three coffee (*Coffea arabica* L.) pulp aqueous extracts. Integr Med Res 5(4): 324–331. https://doi.org/10.1016/j.imr.2016.09.001

Durán-Aranguren DD, Robledo S, Gomez-Restrepo E, Valencia JWA, Tarazona NA (2021) Scientometric overview of coffee by-products and their applications. Molecules 26(24): 7605. https://doi.org/10.3390/molecules26247605

Fitriana N, Rifa'i M, Masruri, Wicaksono ST, Widodo N (2022) Potential of *Curcuma xanthorrhiza* ethanol extract in inhibiting the growth of T47D breast cancer cell line: *In vitro* and bioinformatic approach. J Pharm Pharmacogn Res 10(6): 1015–1025. https://doi.org/10.56499/jppres22.1448_10.6.1015

Gallardo-Ignacio J, Nicasio-Torres MP, Santibáñez A, Cabrera-Hilerio SL, Cruz-Sosa F (2022) Ethnopharmacological study of the genus *Coffea* and compounds of biological importance. Rev Mex Ing Quim 21(3): Bio2856. https://doi.org/10.24275/rmiq/Bio2856

Giaquinto AN, Sung H, Miller KD, Kramer JL, Newman LA, Minihan A, Jemal A, Siegel RL (2022) Breast cancer statistics, 2022. CA Cancer J Clin 72(6): 524–541. https://doi.org/10.3322/caac.21754

Hardjono S, Siswandono, Purwanto, Darmanto W (2016) Quantitative structure-cytotoxic activity relationship 1-(benzoyloxy)urea and its derivative. Curr Drug Discov Technol 13(2): 101–108. https://doi.org/10.2174/1570163813666160525112327

Khochapong W, Ketnawa S, Ogawa Y, Punbusayakul N (2021) Effect of *in vitro* digestion on bioactive compounds, antioxidant and antimicrobial activities of coffee (*Coffea arabica* L.) pulp aqueous extract. Food Chem 348: 129094. https://doi.org/10.1016/j.foodchem.2021.129094

Klingel T, Kremer JI, Gottstein V, de Rezende TR, Schwarz S, Lachenmeier DW (2020) A review of coffee by-products including leaf, flower, cherry, husk, silver skin, and spent

grounds as novel foods within the European Union. Foods 9: 665–685. https://doi.org/10.3390/foods9050665

Li B, Shao H, Gao L, Li H, Sheng H, Zhu L (2022) Nano-drug co-delivery system of natural active ingredients and chemotherapy drugs for cancer treatment: A review. Drug Deliv 29(1): 2130–2161. https://doi.org/10.1080/10717544.2022.2094498

Liu H, Hua Y, Zheng X (2015) Effect of coffee consumption on the risk of gastric cancer: A systematic review and meta-analysis of prospective cohort studies. PloS One 10(5): e0128501. https://doi.org/10.1371/journal.pone.0128501

Love RR, Leventhal H, Easterling DV, Nerenz DR (1989) Side effects and emotional distress during cancer chemotherapy. Cancer 63(3): 604–612. https://doi.org/10.1002/1097-0142(19890201)63:3<604::AID-CNCR2820630334>3.0.CO;2-2

Luzak B, Przemysław S, Boncler M (2022) An evaluation of a new high-sensitivity PrestoBlue assay for measuring cell viability and drug cytotoxicity using EA.hy926 endothelial cells. Toxicol In Vitro 83: 105407. https://doi.org/10.1016/j.tiv.2022.105407

Melosky B, Kambartel K, Häntschel M, Bennetts M, Nickens DJ, Brinkmann J, Kayser A, Moran M, Cappuzzo F (2022) Worldwide prevalence of epidermal growth factor receptor mutations in non-small cell lung cancer: A meta-analysis. Mol Diagnosis Ther 26: 7–18. https://doi.org/10.1007/s40291-021-00563-1

Nur S, Aisyah AN, Lukitaningsih E, Rumiyati, Juhardi RI, Andirah R, Hajar AS (2021) Evaluation of antioxidant and cytotoxic effect against cancer cells line of *Angiopteris ferox* Copel tuber and its compounds by LC-MS analysis. J Appl Pharm Sci 11(8): 54–61. https://doi.org/10.7324/JAPS.2021.110808

Nur S, Hanafi M, Setiawan H, Nursamsiar, Elya B (2023) *In silico* evaluation of the dermal antiaging activity of *Molineria latifolia* (Dryand. ex W.T.Aiton) Herb. Ex Kurz compounds. J Pharm Pharmacogn Res 11(2): 325–345. https://doi.org/10.56499/jppres23.1606_11.2.325

Nursamsiar, Nur S, Febrina E, Asnawi A, Syafiie S (2022) Synthesis and inhibitory activity of curculigoside A derivatives as potential anti-diabetic agents with β-cell apoptosis. J Mol Struct 1265: 133292. https://doi.org/10.1016/j.molstruc.2022.133292

Nursamsiar, Siregar M, Awaluddin A, Nurnahari N, Nur S, Febrina E, Asnawi A (2020) Molecular docking and molecular dynamic simulation of the aglycone of curculigoside a and its derivatives as alpha glucosidase inhibitors. Rasayan J Chem 13(1): 690–698. https://doi.org/10.31788/RJC.2020.1315577

Ramírez D, Caballero J (2018) Is it reliable to take the molecular docking top scoring position as the best solution without considering available structural data? Molecules 23(5): 1038. https://doi.org/10.3390/molecules23051038

Rios MB, Iriondo-DeHond A, Iriondo-DeHond M, Herrera T, Velasco D, Gómez-Alonso S, Callejo MJ, Del Castillo MD (2020) Effect of coffee cascara dietary fiber on the physicochemical, nutritional and sensory properties of a gluten-free bread formulation. Molecules 25(6): 1358. https://doi.org/10.3390/molecules25061358

Riwu AG, Nugraha J, Purwanto DA, Triyono EA (2022) *In silico* analysis of anti-dengue activity of faloak (*Sterculia quadrifida* R. Br) stem bark compounds. J Pharm Pharmacogn Res 10: 1006–1014. https://doi.org/10.56499/jppres22.1445_10.6.1006

Rosandy AR, Ishak SSO, Sabri NA, Yaacob WA, Al Muqarrabun LMR (2021) Antibacterial activity of lupeol from the bark of *Dehaasia cuneate* (Lauraceae). Curr Res Biosci Biotechnol 2(2): 145–148. https://doi.org/10.5614/crbb.2021.2.2/BOFY6724

Rosandy AR, Ying YC, Kqueen CY, Lim SJ, Latip J, Murad AMA, Bakar MA, Khalid RM (2018) (-) Glaciantarcin, a new dipeptide and some secondary metabolites from the psychrophilic yeast *Glaciozyma antarctica* PI12. Sains Malays 47(11): 2693–2698. http://dx.doi.org/10.17576/jsm-2018-4711-12

Schegoleva AA, Khozyainova AA, Gerashchenko TS, Zhuikova LD, Evgeny VD (2022) Metastasis prevention: Targeting causes and roots. Clin Exp Metastasis 39: 505–519. https://doi.org/10.1007/s10585-022-10162-x

Silva MO, Honfoga JNB, de Medeiros LL, Madruga MS, Bezerra TKA (2021) Obtaining bioactive compounds from the coffee husk (*Coffea arabica* L.) using different extraction methods. Molecules 26: 46. https://doi.org/10.3390/molecules26010046

Tan H, Zhao C, Zhu Q, Katakura Y, Tanaka H, Ohnuki K, Shimizu K (2019) Ursolic acid isolated from the leaves of loquat (*Eriobotrya japonica*) inhibited osteoclast differentiation through targeting exportin 5. J Agric Food Chem 67(12): 3333–3340. https://doi.org/10.1021/acs.jafc.8b06954

Yashin A, Yashin Y, Xia X, Nemzer B (2017) Chromatographic methods for coffee analysis: A review. J Food Res 6(4): 60–82. https://doi.org/10.5539/jfr.v6n4p60

AUTHOR CONTRIBUTION:

Contribution	Novi F	Berna E	Hayun	Kusmardi K
Concepts or ideas	x	x	x	x
Design	x	x	x	x
Definition of intellectual content	x	x	x	x
Literature search	x	x		
Experimental studies	x	x	x	
Data acquisition	x	x	x	x
Data analysis	x		x	x
Statistical analysis	x		x	
Manuscript preparation	x	x	x	
Manuscript editing	x		x	
Manuscript review	x	x	x	x

Citation Format: Novi F, Berna E, Hayun, Kusmardi K (2024) Structure elucidation of active compounds from *Coffea canephora* Pierre ex A.Froehner cascara and their potential as anticancer against breast cancer cells. J Pharm Pharmacogn Res 12(1): 73–90. https://doi.org/10.56499/jppres23.1735_12.1.73

Supplementary data

Figure S1. Structural chromatographic elucidation of lupeol.

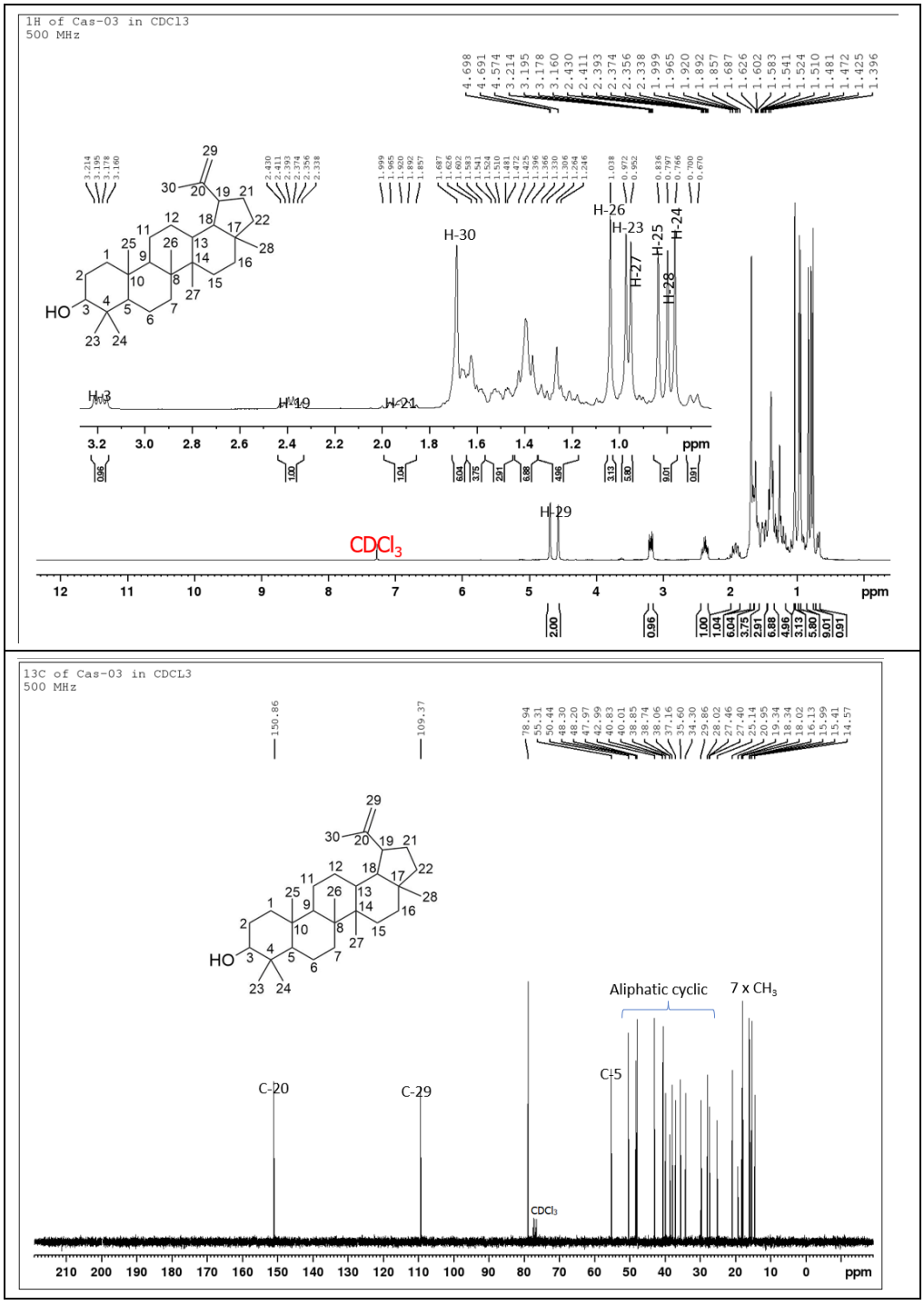

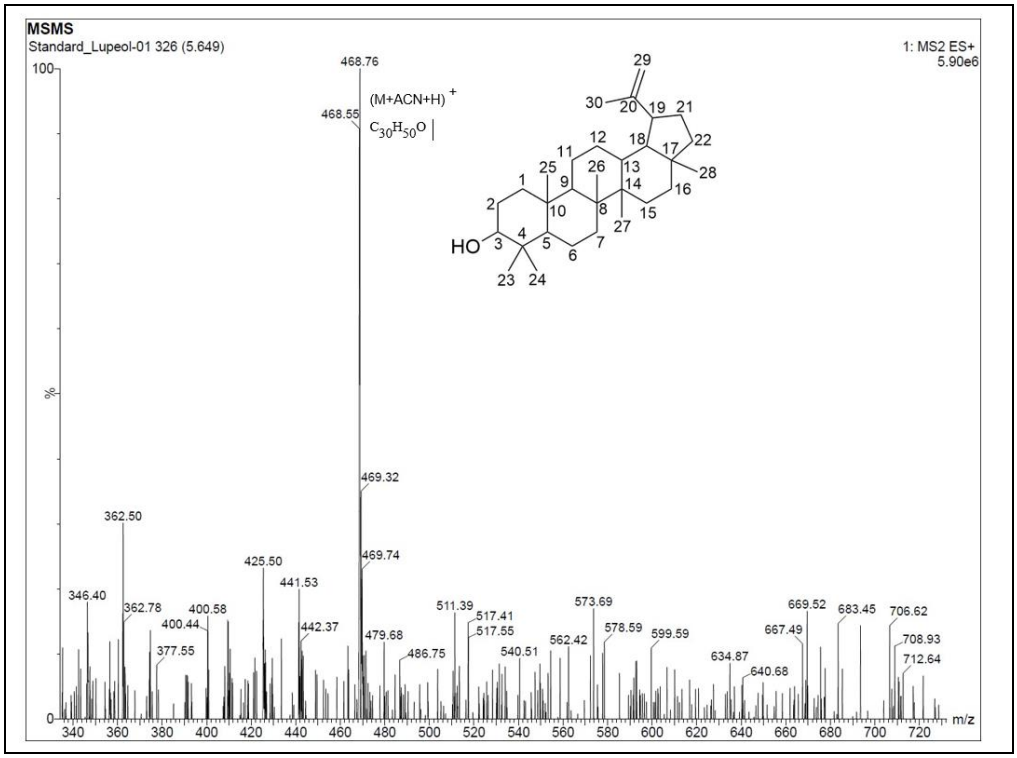

Figure S2. Structural chromatographic elucidation of stigmasterol.

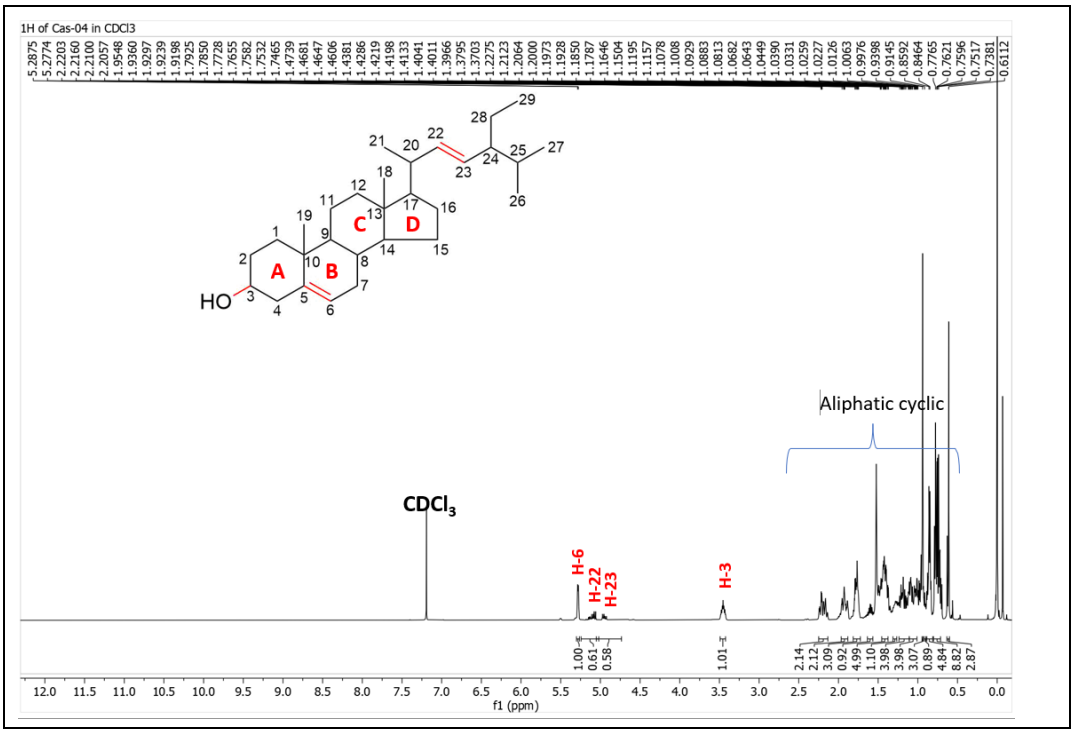

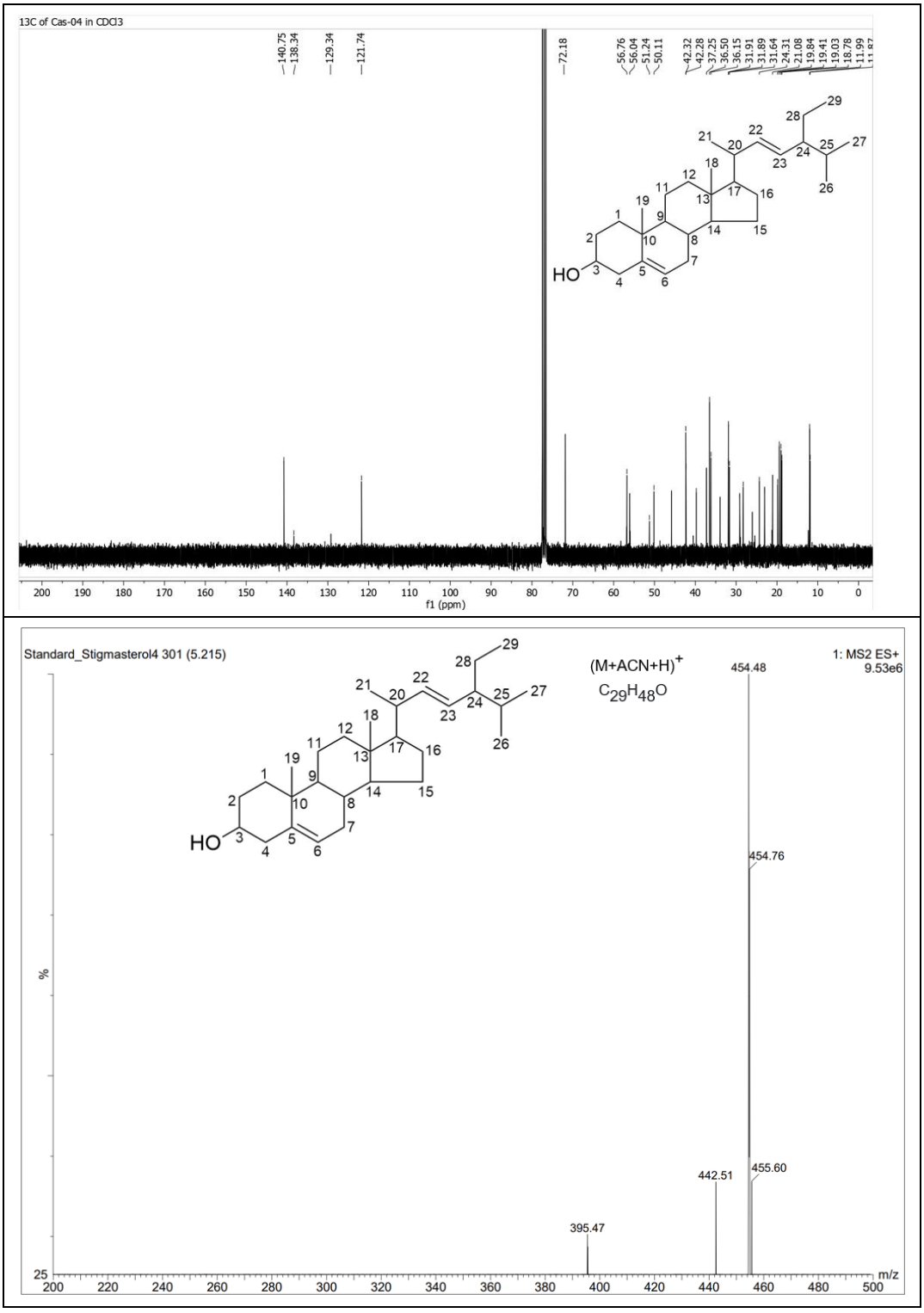
13C of Cas-04 in CDCl3
140.75
138.34
129.34
121.74
72.18
56.76
56.04
51.24
50.11
42.32
42.28
37.25
36.50
36.15
31.91
31.89
31.64
24.31
21.08
19.84
19.41
19.03
18.78
11.99
HO
f1 (ppm)
Standard_Stigmasterol4 301 (5.215)
(M+ACN+H)+
C29H48O
1: MS2 ES+
9.53e6
454.48
454.76
455.60
442.51
395.47
%
m/z

Figure S3. Structural chromatographic elucidation of ursolic acid.

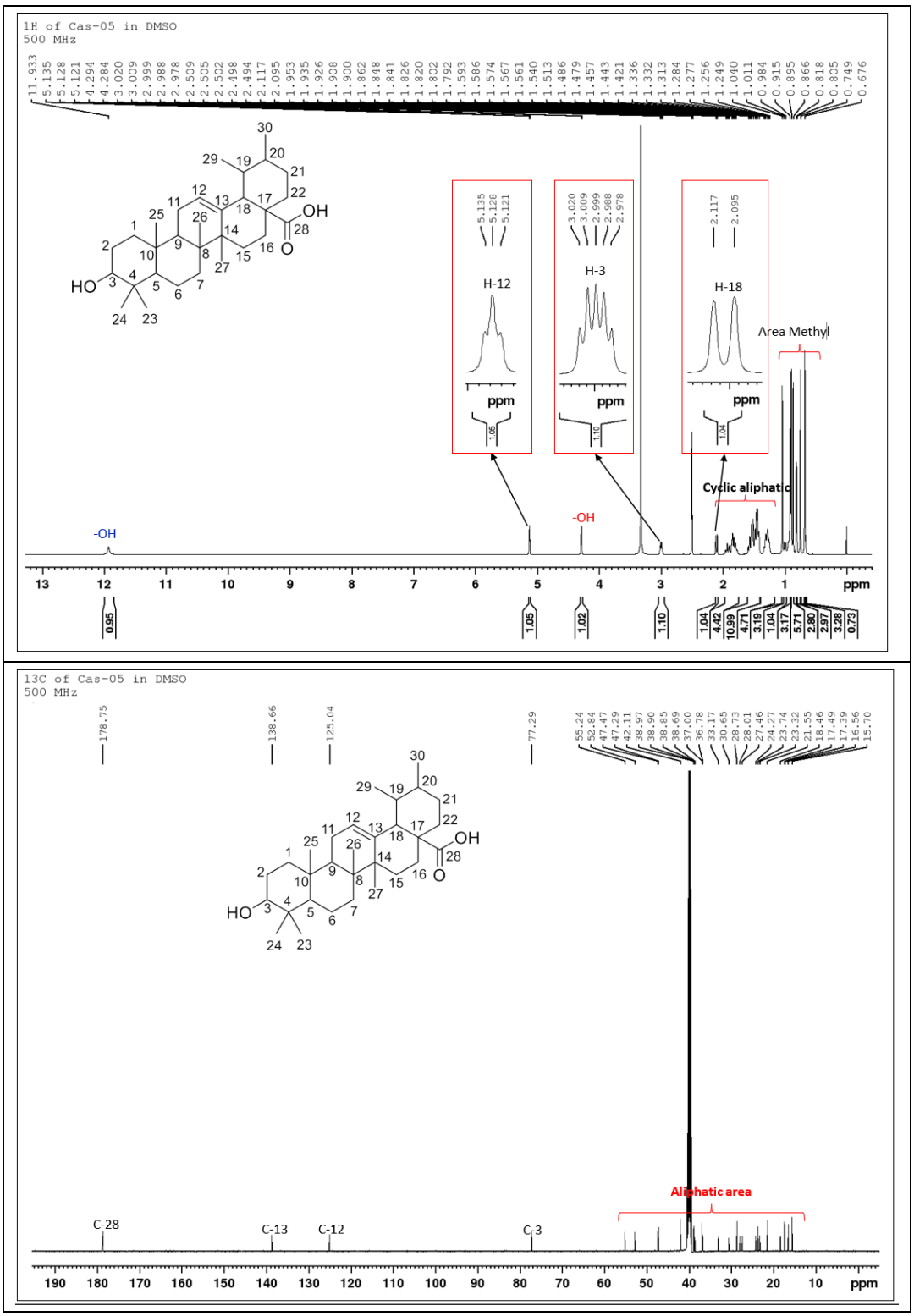

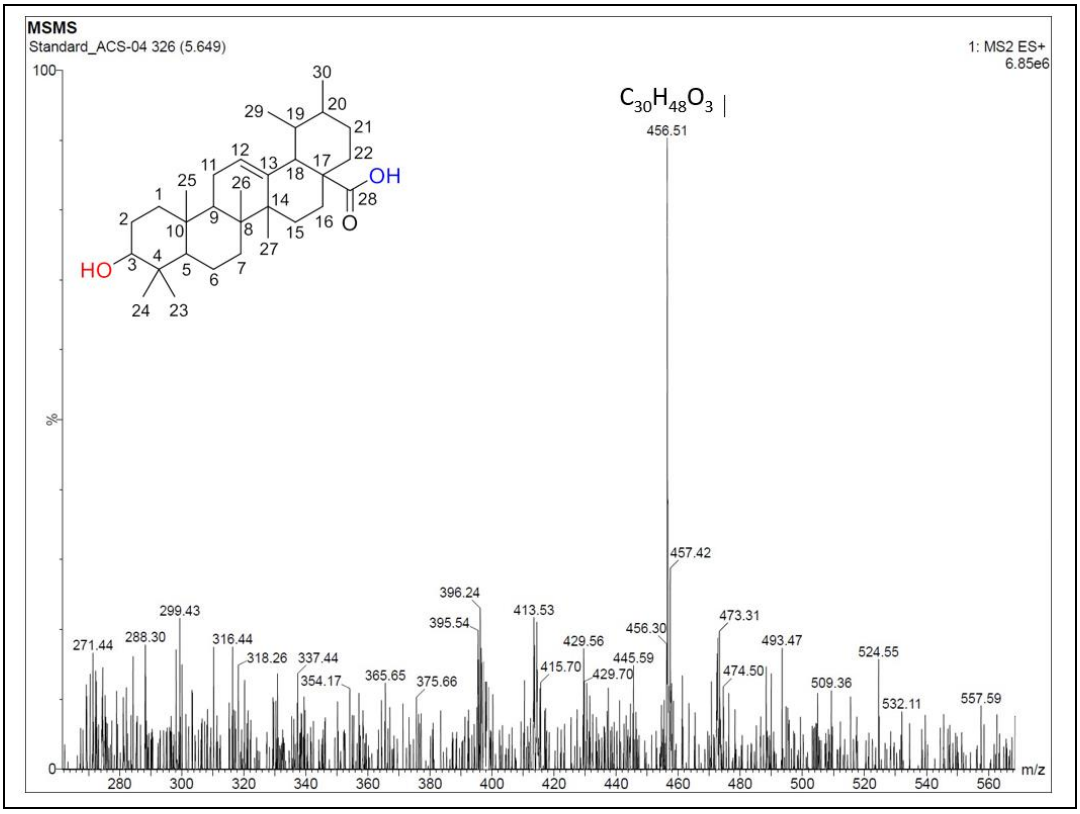

Figure S4. Structural chromatographic elucidation of caffeic acid.

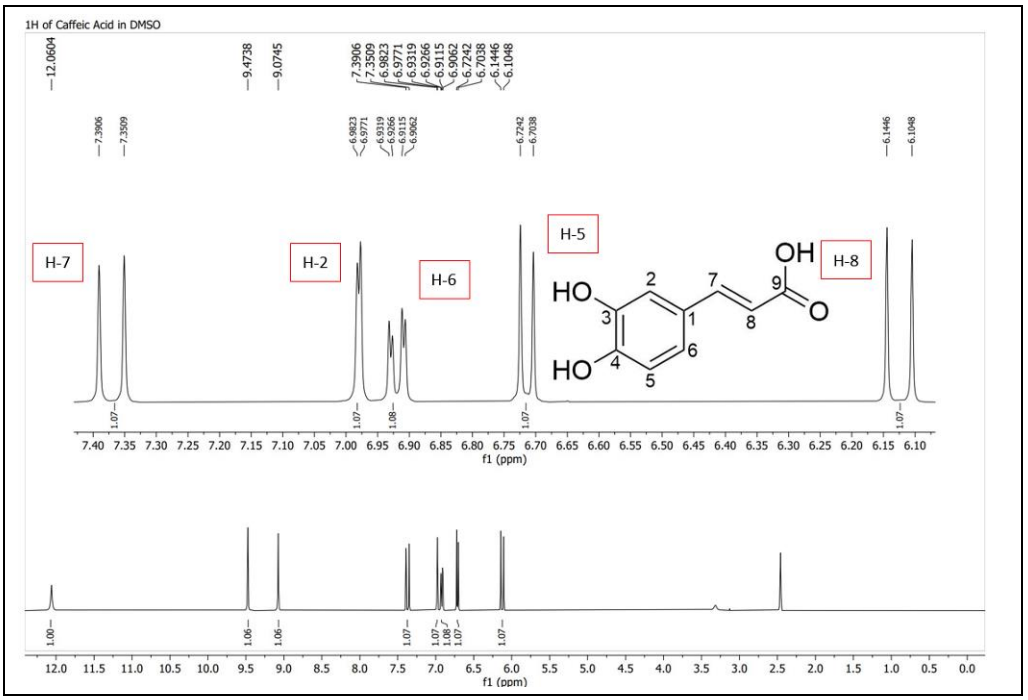

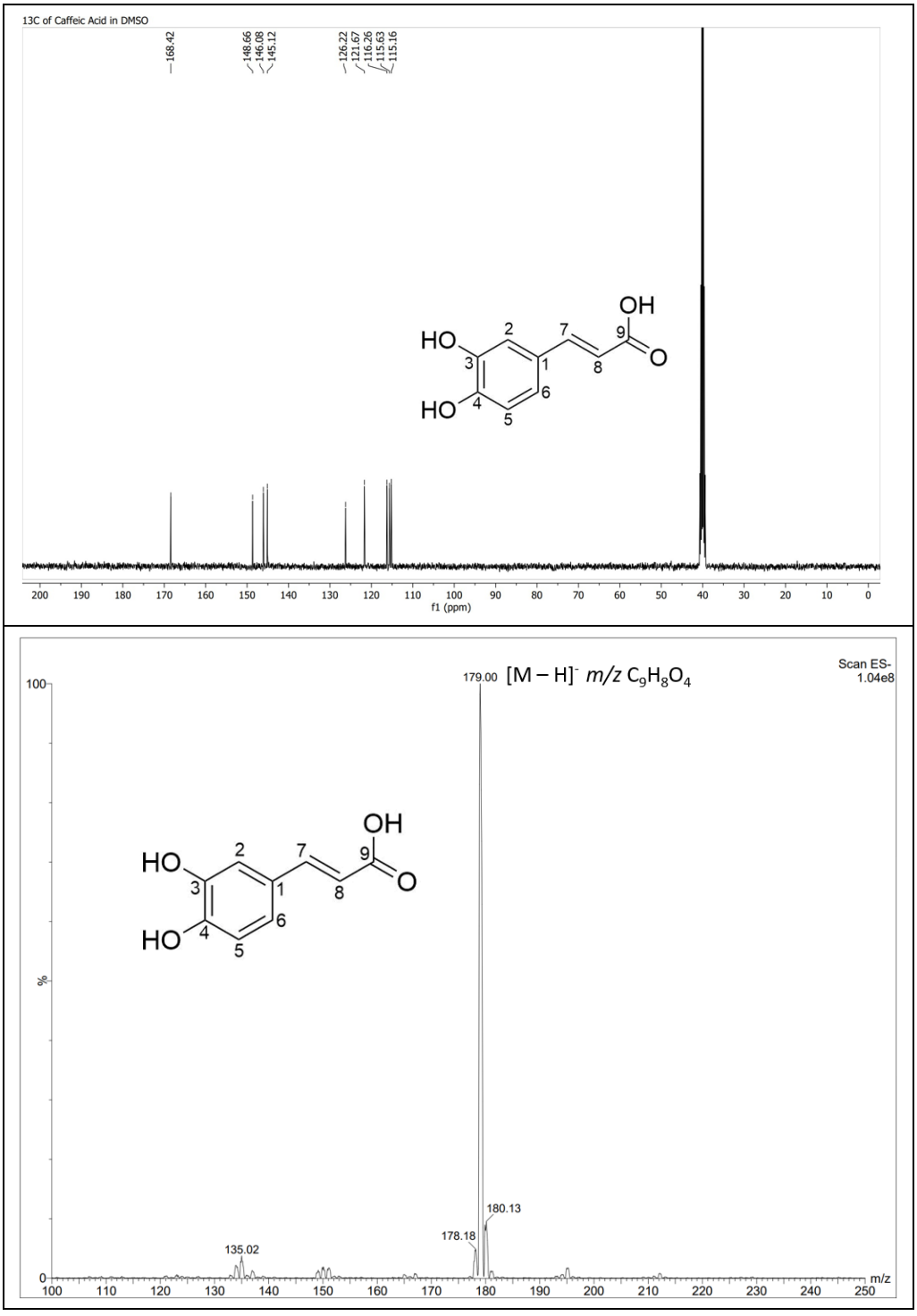
13C of Caffeic Acid in DMSO
168.42
148.66
146.08
145.12
126.22
121.67
116.26
115.63
115.16
HO
HO
OH
O
f1 (ppm)
Scan ES-
1.04e8
179.00 [M – H]⁻ m/z C9H8O4
100
%
0
180.13
178.18
135.02
m/z